X-810-72-177
PREPRINT

NASA TM X-66092

VERY HIGH-FREQUENCY (VHF) IONOSPHERIC SCINTILLATION FADING MEASUREMENTS AT LIMA, PERU

MAY 1972

GSFC

GODDARD SPACE FLIGHT CENTER

GREENBELT, MARYLAND

X-810-72-177

VERY HIGH-FREQUENCY (VHF) IONOSPHERIC SCINTILLATION FADING MEASUREMENTS AT LIMA, PERU*

Howard A. Blank**

Thomas S. Golden
Network Engineering Division

May 1972

* Presented April 13-15, 1972, at 1972 USNC/URSI – IEEE Spring Meeting, Washington, D.C.
** Computer Sciences Corporation

GODDARD SPACE FLIGHT CENTER
Greenbelt, Maryland

VERY HIGH-FREQUENCY (VHF) IONOSPHERIC SCINTILLATION FADING MEASUREMENTS AT LIMA, PERU

Howard A. Blank
Thomas S. Golden

ABSTRACT

During the spring equinox of 1970, scintillating signals at VHF (136.4 MHz) were observed at Lima, Peru. The transmission originated from ATS 3 and was observed through a pair of antennas spaced 1200 feet apart on an east-west baseline. The empirical data have been digitized, reduced, and analyzed utilizing the computer center at NASA/GSFC. The results of that analysis are presented in this report. They include amplitude probability density and distribution functions, time autocorrelation functions, cross-correlation functions for the spaced antennas, and appropriate spectral-density functions. The presentation of the results of the analysis shows estimates of the statistics of the ground diffraction pattern to gain insight into gross ionospheric irregularity size, and irregularity velocity in the plane of the antennas.

CONTENTS

ILLUSTRATIONS

ILLUSTRATIONS (continued)

For several years, the occurrence of scintillation fading of transionospheric VHF signals in the equatorial region has been recognized. Fading effects have been shown to degrade VHF telemetry and tracking functions in the NASA stations in South America.

Occurrence of fading is most predominant around the spring and fall equinoxes and is usually restricted to early evening hours. Intensity and duration of fading decreases as the observer moves from the geomagnetic equator to approximately ±25 degrees latitude.

The work of Kent and Koster[1], Pomalaza, et al.,[2] and Golden[3] led to the suggestion of space diversity as a means of overcoming degradation of telemetry.

A pair of VHF antennas spaced 1200 feet apart on a west-east baseline have been used for recording some 75 hours of beacon data at Lima, Peru, on the geomagnetic equator. Data were collected during the early evening hours from December 12, 1969 to April 19, 1970. The bulk of the reduced and analyzed data was collected just after the occurrence of the spring equinox (Figure 1); some typical results of processing this data are presented.

This report is organized into five parts. Following the introduction, a brief description of the experiment is presented. The satellite transmitter and spaced ground receiver configuration are discussed. The data-conversion and reduction procedure is described next. Details of some of the results of the data reduction and analysis are then presented. Specifically, a complete collection of the statistical functions obtained for two representative data-collection runs is shown, and the results discussed. In addition, the results of an analysis to determine the average west-east ground diffraction pattern velocity and size are presented. Supporting probability density functions of auto- and cross-correlation functions are also shown. The last part summarizes the results found from this experiment.

EXPERIMENT DESCRIPTION

VHF (136.470 MHz) signals from the ATS-3 synchronous satellite were received by the Geophysical Institute of Peru satellite tracking station at Lima (Ancon), Peru. This was chosen as the data-collection site because of its location on the geomagnetic equator, the availability of receiving and data-collection equipment, and the presence of interested ionospheric researchers. The geographical location of Ancon, Peru, is 79° 9' 1.77"W latitude and 11° 46' 44.43"S longitude. The elevation angle to ATS 3 was approximately 72 degrees.

The ATS-3 spacecraft is spin-stabilized in a synchronous equatorial orbit; it is located approximately 70° W longitude, which is over the eastern Pacific Ocean and near the west coast of Mexico. The spacecraft antenna used for tracking, telemetry, and command consists of an eight-whip turnstile, and is essentially omnidirectional. The overall effective radiated power (ERP) of the satellite is 25.8 dBW.

The receiver site configuration (Figure 2) consists of two receiving antennas separated on a 1200-foot west-east baseline, a cable run from each antenna to the receiver building, two receivers, and appropriate data recording equipment. Specifically, as shown in Figure 3, each VHF receiver system consists of a Taco-9 element Yagi antenna (right-hand circular polarized), appropriate preamplifiers, Bendix Modification I receivers, and interstate tracking filters. The VHF signal level, as represented by the coherent AGC of the tracking filters, was recorded on both a Sanborn strip-chart recorder and an Ampex FR600 magnetic tape recorder, simultaneously. The receivers operated at a nominal received carrier level of about -123.1 dBm.

The VHF carrier at the east antenna was connected to receiver Channel A of Modification I, and the VHF carrier at the west antenna was connected to Channel B. The IF bandwidth was 10 kHz, and the carrier was tracked in a 30-Hz bandwidth, yielding a C-to-N (carrier-to-noise) ratio of 35 dB. This is sufficient to track the carrier for fades of up to -27 dB.

It was desired to record a linear AGC. Thus, the FR600 was set up such that +1.4 volts represented -80 dBm, and -1.4 volts represented -130 dBm. The magnetic tape speed was set at 3.75 inches per second, and the paper tape recorder was set at various speeds, depending on the level of scintillation activity. All magnetic tape recordings of the coherent AGC were made in the FM mode.

DATA REDUCTION

The data-conversion and reduction procedure is shown in Figure 4. All of the equipment involved is located at GSFC. All data processing was conducted using this equipment.

Three basic steps are used in the computer processing of data. The first step is to digitize the analog recording collected in the field. The second step is to interpret and translate the digitized levels to obtain a time series of signal strength measurements. The third step is to extract the desired statistics from the translated time series.

The analog tapes recorded in the field are multichannel. Two channels contain FM information, where the modulating signals are the voltage levels of the AGC circuits of the two space-diversity receivers. Other channels have voice information (operator comments), a continuous tone of fixed frequency for tape servostabilization, and a continuous time code.

When a tape is to be processed, it is positioned using the time code, then played back at eight times the recording speed (using tape servo). The voltage outputs from the circuits detecting the FM signals (the AGC data) are fed to an analog-to-digital converter which has a resolution of 16384 levels (14 bits). The output of the A/D converter, consisting of a sequence of pairs of 14-bit words (each pair being one sample of both receivers), is rearranged for writing on a standard computer tape.

According to instructions, the operator in the field is to use test equipment to record a set of calibrated signal levels before the received signal is recorded, one calibration sequence per channel. This entire routine was digitized in the previous step; therefore, a program is necessary to interpret the precalibration sequences and use the results to translate the remaining data into two time series of signal strength measurements.

Calibration of the data is by linear interpolation between analog calibration steps.* For example, a digital level of 12192 would have been translated as -88.38 dBm from the above precalibration. Alternatively, the process has been arranged so that this level would have been translated as 1.453×10^{-10} milliwatts, the output units being selected at execution time.

Whatever the units, the translated signal strength pairs are written on a nine-track computer tape. The sampling rate for this analysis was 200 samples per second; therefore, one physical record on the output tape contains 5 seconds of samples of each receiver.

The following list of analysis programs were written for the reduction of the field data:

- Probability Density Function vs Signal Level (dBm or mw)
- Probability Distribution Function vs Signal Level (dBm or mw)

*This does not imply that equal analog-power-level steps will translate to equal numbers of digital levels.

- Autocorrelation Function vs Time Lag (sec)
- Crosscorrelation Function vs Time Lag (sec)
- Spectral-Density Function vs Frequency (Hz)
- Level-Crossing Distribution Function vs Signal Level (dBm or mw)

These programs are broken into two main packages. They use the nine-track tapes produced in step two as input. The distribution program can analyze different time spans of data (skipping certain time spans) as desired. For each time span and channel, a density function (pdf) and a cumulative distribution function (cdf) are produced on the printer or CalComp plotter. Also printed are the third-peak scintillation index ($S.I._0$), the coefficient variation scintillation index ($S.I._4$), and the sum and sum-of-squares of the signal strengths for possible use in other scintillation index formulas. If desired, the mean signal strengths for each channel and time span may be saved temporarily, the input tape rewound, and the same time spans reanalyzed for fade duration statistics. In this case, the pdf and cdf of the fade duration below various thresholds less than the mean signal strength are plotted. This program treats every pair of points during the analysis of a given time span. The other is the correlation program, which will again analyze selected time spans of data, both printing and plotting the auto- and crosscorrelation functions and the spectral-density function for each channel. The spectral density may also be filtered with one or more spectral windows, the narrowest window having a width one-twentieth the total length of the selected time span. Note that this program has the option of skipping sample pairs, thus allowing a simulation of a slower sampling.

DATA PRESENTATION

The statistics obtained from two representative data-collection runs are shown in Figures 5 through 9. Run 38/2 consisted of 46 minutes of data, collected on April 2, 1970. The analyzed results are representative of 14 minutes of these data. Run 56A/1 consisted of 33 minutes of data, collected on April 13, 1970. The analyzed results are representative of 28 minutes of these data.

The probability density functions of runs 38/2 and 56A/1 are shown in Figure 5. These are plotted as frequency-of-occurrence of a received power level versus that power level in dBm. The figure also shows the mean, standard deviation, and two scintillation indices associated with the run. Each plot represents the probability density function of analog data sampled at 200 samples per second.

Figure 6 shows plots of the cumulative probability distribution functions corresponding to each of the probability density functions of Figure 5. Each distribution function is plotted as the cumulative probability of a signal level being exceeded versus that signal level in dBm. Note that the probability is scaled according to a Gaussian variate. That is, the cumulative probability distribution function of a Gaussian random process will appear as a straight line with its mean value at the 50-percent point.

Figure 7 shows plots of the autocorrelation functions of runs 38/2 and 56A/1. Each function is plotted as the normalized autocorrelation function versus time lag in seconds. The autocorrelation functions were calculated from data sampled at 10 samples per second. The sampling rates were selected on the basis of 10 times the expected fading rate. The shape of the autocorrelation functions can be interpreted to imply a number of phenomena. For example, if coherent time period $t + \tau$ is selected (i.e., that value of τ during which the autocorrelation falls from a value of unity to a value less than unity, say 0.5) and signals received beyond that period are considered to be independent of the received signal at t, an estimate of gross diffraction pattern size may be made if the west-east diffraction pattern velocity is known. The latter quantity may be obtained by analysis of the corresponding crosscorrelation function. Another parameter that may be gleaned from the autocorrelation function is the average fading rate, or Doppler spread. This can be obtained by taking the inverse of the coherent time directly or by taking the Fourier transform of the autocorrelation function (i.e., the spectral density) and using elements of circuit theory analysis to determine the fading rate.

The crosscorrelation functions between the west and east antennas for runs 38/2 and 56A/1 are shown in Figure 8. Each function is plotted as the normalized crosscorrelation function versus time delay in seconds. As in the case of the autocorrelation functions, the crosscorrelation functions were calculated on the basis of 10 times the expected fading rate. The crosscorrelation functions obtained in this experiment are measures of the similarity of the received stochastic processes observed at two antennas separated by 332 meters (1200 feet) on a west-east baseline and pointed at the same satellite signal source. Although ionospheric motion gives rise to a dominant west-east component for the diffraction pattern, it is well known that there is also considerable movement in the other degrees of freedom, Clemesha.[4] That significant north-south, vertical, and small-scale turbulences may also exist is seen by observing the values of the positive peaks of the crosscorrelation functions. Probability $P(Y(t + \tau) = A \mid x(t) = A_{max})$, where x(t) is the received random signal for the west antenna and y(t) is the received random signal for the east antenna, is always less than unity. This value has extremes. For example, the peak crosscorrelation coefficient for run 56A/1 is .947, whereas the peak crosscorrelation coefficient for run 38/2 is 0.950. Other runs, not shown, have even wider

variations in crosscorrelation behavior. Examples are run 14/1, collected on January 6, 1970, and Run 21/1, collected on January 24, 1970. The peak cross-correlation coefficient of the former is 0.345, and that of the latter is -.180.

Factors other than motion in non-west-east degrees of freedom are recognized for contributing to the variation in the value of the peak crosscorrelation coefficient. Transmission through multiple layers may be a factor.[2] In particular, the extremely low-peak crosscorrelation coefficient observed for run 21/1 may need further investigation. However, due to the generally high values of peak crosscorrelation coefficients obtained from the data collected during the course of this experiment (i.e., average peak crosscorrelation coefficient was 0.939), it is believed that valuable information may be obtained about the west-east movement and size of equatorial ionospheric gross irregularities.

Figure 9 shows the spectral-density functions of runs 38/2 and 56A/1. They are plotted as spectral power versus frequency in Hz. Each spectral-density function is the direct Fourier transform of its corresponding autocorrelation function. These functions yield information pertaining to the Doppler spread characteristics of the scintillating medium. Using elements of circuit theory, the fading bandwidth of the medium is defined as that frequency for which the spectral power is one-half its zero-frequency (i.e., dc) value. The zero-frequency value is indicated by an "X" on the ordinate of the plot. The spectral-density functions shown have been smoothed by a "Hanning" (i.e., "Tukey")[5] spectral window.

This paragraph is a preliminary analysis of gross irregularity size and average west-east velocity based on the results obtained from the computer-processed statistical functions. Each autocorrelation function of the data runs of this experiment was analyzed to obtain the time delay (in seconds) corresponding to the following correlation values:

- 0.5
- 0.3
- 0.1

Those correlation functions that represented little or no scintillation activity (i.e., those with extremely long-correlation times) were eliminated from the analysis to avoid biasing the results. Figure 10 shows the probability density function of the random variable representing the time at which an autocorrelation coefficient of 0.5 second occurred. The figure also shows the corresponding probability density function for the 0.3 coefficient, and the density function for the 0.1 coefficient. With the exception of the mean values of the 0.5 and 0.3

functions, it appears that the two would be similarly distributed. The 0.1 function, however, is of a different nature. Such a result is expected because the 0.5 and 0.3 coefficients are generally in the body of the autocorrelation functions, and the 0.1 coefficient is generally near the "tail" of the autocorrelation functions. Given the average west-east velocity of the ionospheric diffraction patterns, the probability density functions of Figure 10 can be used to estimate gross irregularity size. The average west-east velocity, as we shall see, can be estimated from the crosscorrelation functions.

Figure 11 shows the probability density function of the peak value of the crosscorrelation functions for the runs of this experiment (30 runs were included). The average peak value is 0.939, indicating that the diffraction pattern tends to hold its basic gross shape as it drifts between the two antennas. Figure 12 shows the probability density function of the delay times corresponding to the peak values of the crosscorrelation functions. The average value of the delay of the peak of the crosscorrelation functions is 2.48 seconds. The antennas being 1200 feet apart implies an average west-east velocity of 484 feet per second (147 m/s) for ionospheric irregularities during the course of this experiment. Figure 12 also shows that the probability density function of the delays of the peak crosscorrelation values is primarily distributed near its mean value. Therefore, selecting the mean delay as representative is appropriate.

The mean value of the probability density function of the 0.5-autocorrelation function (Figure 10) is representative of the "rigidity" of the average ionospheric diffraction pattern. That is, taking twice the time lag over which the autocorrelation functions have average coefficients of at least 0.5, and multiplying by the average west-east velocity, an estimate of the gross west-east dimension of the diffraction pattern is obtained. For the experimental data collected and analyzed during the course of this experiment, the average west-east pattern size is 515 meters. Defining an autocorrelation of 0.3 as representative of the "rigidity" of the irregularity, a west-east irregularity size of 794 meters is obtained. Using an autocorrelation of 0.1, a west-east irregularity size of 1145 meters is obtained.

The previously used straightforward method of computing gross pattern size and west-east average velocity can be improved. The most direct method is to collect data from at least three well-placed antenna locations for a predetermined interval, and form the appropriate crosscorrelation functions. Using these functions and the known distance between the pairs of antennas, the irregularity velocity component along the lines joining the pairs can be determined. Much work has been done to relate the relative components to the true irregularity velocity. Fooks[6] summarized much of the work in the field, and developed a method to obtain the true irregularity (i.e., diffraction pattern)

velocity. Although the experiment described in this paper had only two observing antennas, Fooks' method was applied to obtain a comparison result, and to obtain a measure of the influence of the "rigidity" of the diffraction pattern.

Fooks' method is sensitive to the "decorrelation" implied by the magnitude of the peak crosscorrelation coefficient as compared to unity. The time lag of the autocorrelation function to reach this value from unity is included in the delay time used to determine the average west-east diffraction pattern motion. The results obtained from Fooks' method are nearly the same as gleaned by the simple method previously described. The average peak crosscorrelation coefficient of 0.939 appears to account for about 2 meters per second in the west-east velocity.

The results of west-east scale sizes of diffraction patterns (and the drift velocities), peak crosscorrelation coefficients, and delay times compare favorably with those reported by Pomalaza[2] from a related experiment.

SUMMARY

The results of this experimental effort have produced statistics that represent nocturnal equatorial ionospheric scintillation activity during the spring equinox. A representative segment of the data collected in the field was analyzed to obtain first- and second-order statistical functions that are useful in characterizing the fading behavior of the channel. In particular, the autocorrelation functions of each received signal, coupled with the crosscorrelation functions of signals received on spaced antennas, were used to estimate the west-east average velocity and size of the ground-diffraction pattern. The results are in close agreement with those to be found in the literature. Hopefully, these results will be useful in future studies of gross ionospheric irregularity size and motion. Furthermore, the results presented herein are believed to be useful to those researchers interested in using channel-fading characteristics to design systems in order to avoid their negative effects. Specifically, tracking and telemetry-system designers may take advantage of the space-diversity information presented in order to avoid the effects of ionospheric scintillation. Based on these data, a VHF space-diversity system has been installed at the NASA tracking station at Quito, Equador.

The authors would like to extend their appreciation to Mr. Robert Nelson of the National Aeronautics and Space Administration for designing much of the data-reduction and analysis system used for this experiment. Acknowledgment is also due Mr. Peter Carlston of the Computer Sciences Corporation for completing the design of the system, and supervising the production phase of the data reduction.

REFERENCES

1. G. S. Kent and J. R. Koster. "Some Studies of Night-Time F Layer Irregularities at the Equator Using VHF Signals Radiated from Earth Satellites" from Spread F and Its Effects Upon Radio Propagation. Edited by P. Newman. W. & J. MacKay Co. London. 1966. Chapter 2-6

2. J. Pomalaza, et al. "A Progress Report on Scintillation Observations at Ancon and Jicamarca Observatories." GSFC X-520-70-398. October 1970

3. T. S. Golden. "A Note on Correlation Distance of VHF Fading From Irregularities in the Equatorial Ionosphere." Radio Science. Vol. 5, No. 6. June 1970

4. B. R. Clemesha and W. H. Wright. "A Survey of Equatorial Spread F" from Spread F and Its Effects. Edited by P. Newman. Technivision. Maidenhead, England. 1966. Chapter 1-1

5. R. B. Blackman and J. W. Tukey. "The Measurement of Power Spectra." Dover. 1958

6. G. F. Fooks. "Ionospheric Drift Measurements Using Correlation Analysis Methods of Computation and Interpretation of Results." J. Atm. Terr. Phys. No. 27. 1965. p 979

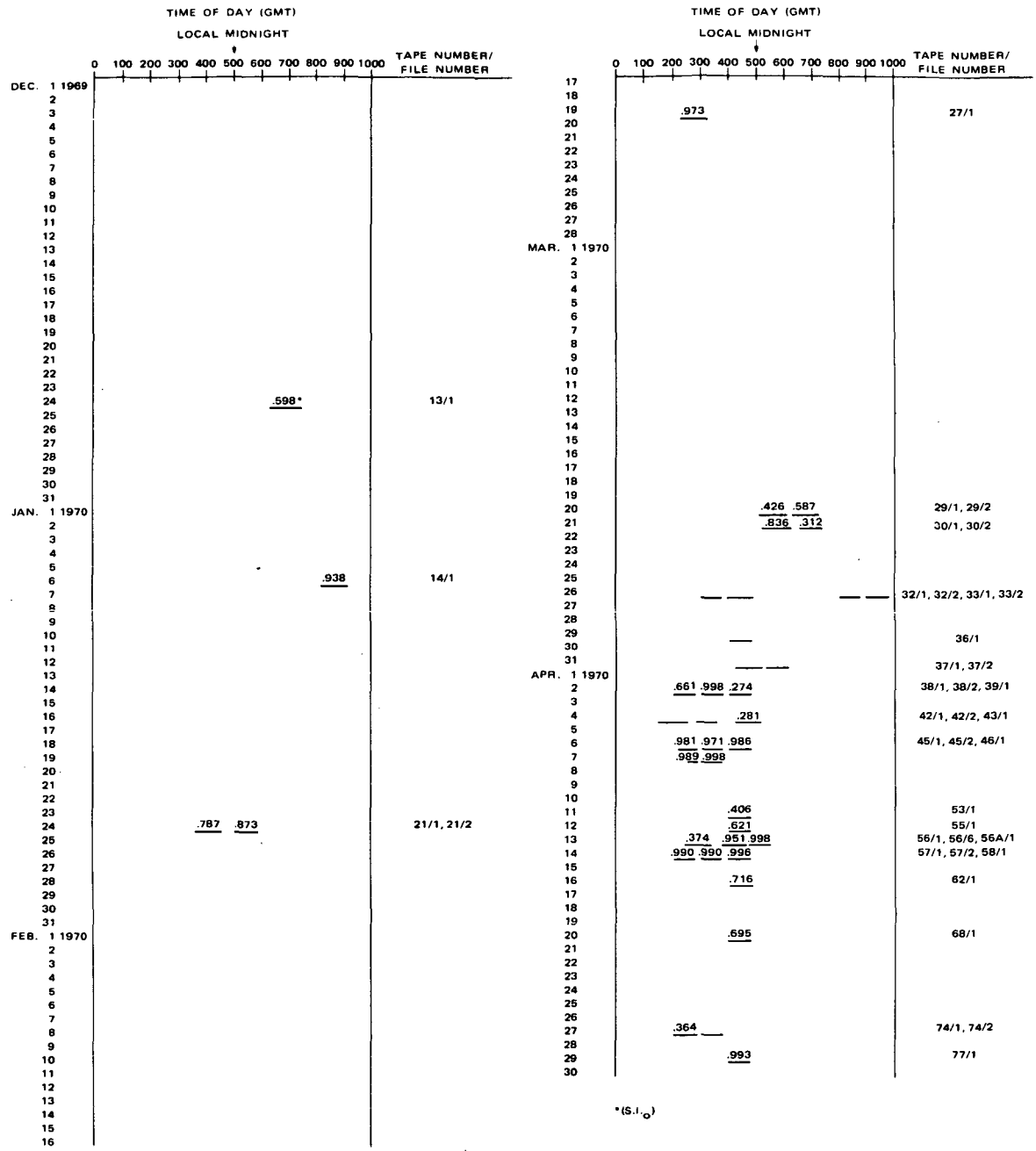

Figure 1. Summary of Data Runs Analyzed

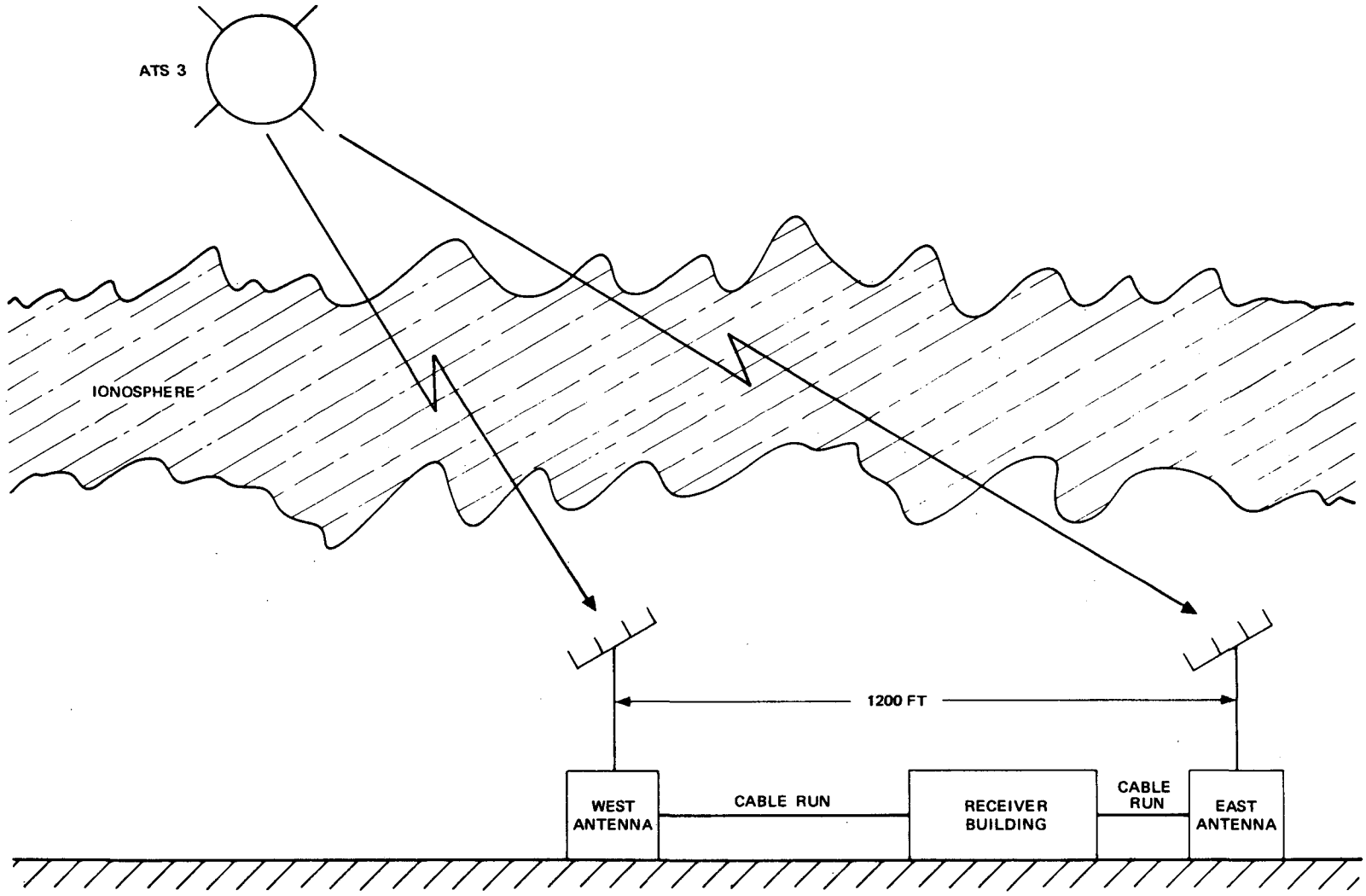

Figure 2. Lima Test Configuration

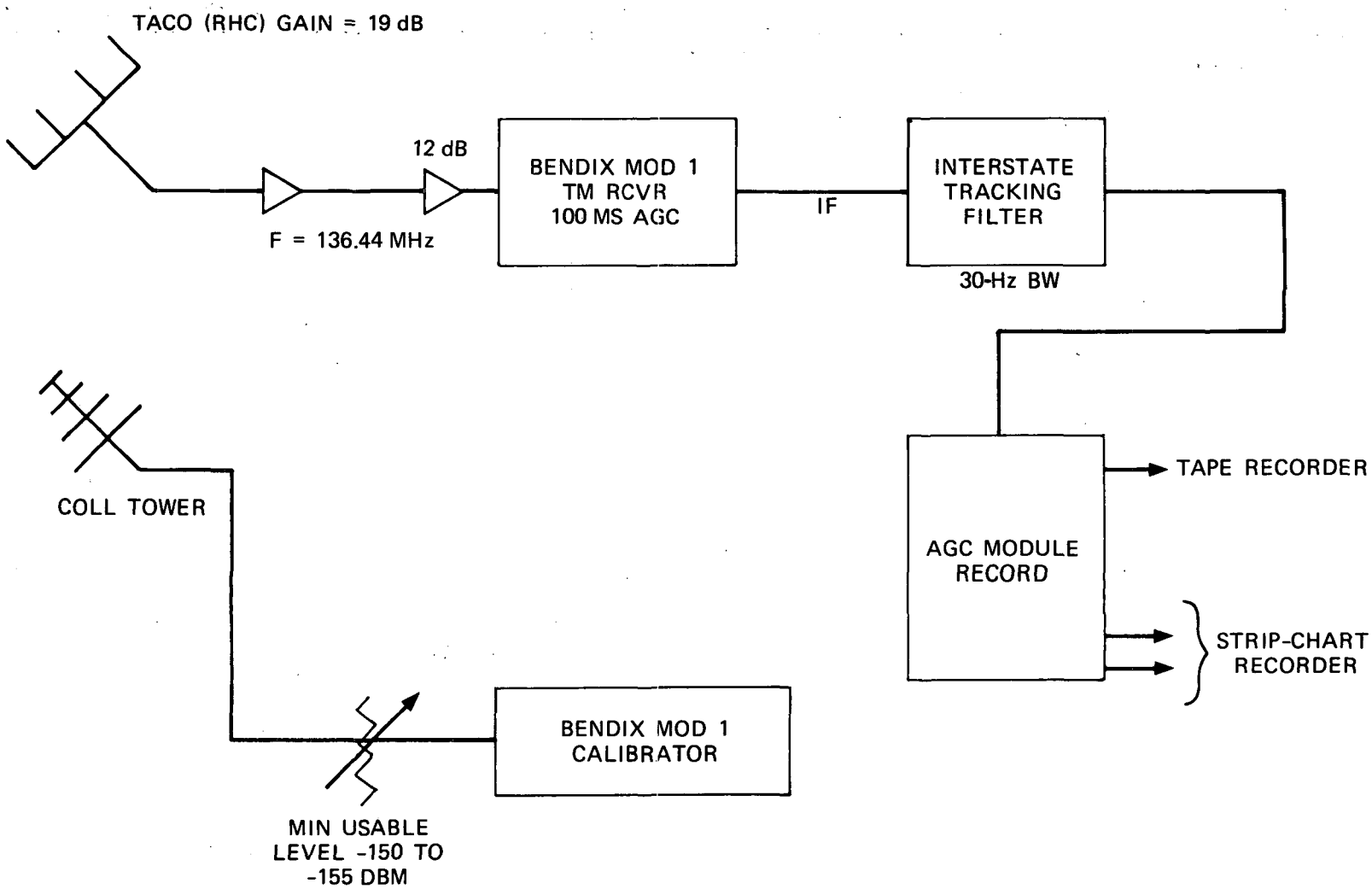

Figure 3. Lima Receiver Configuration

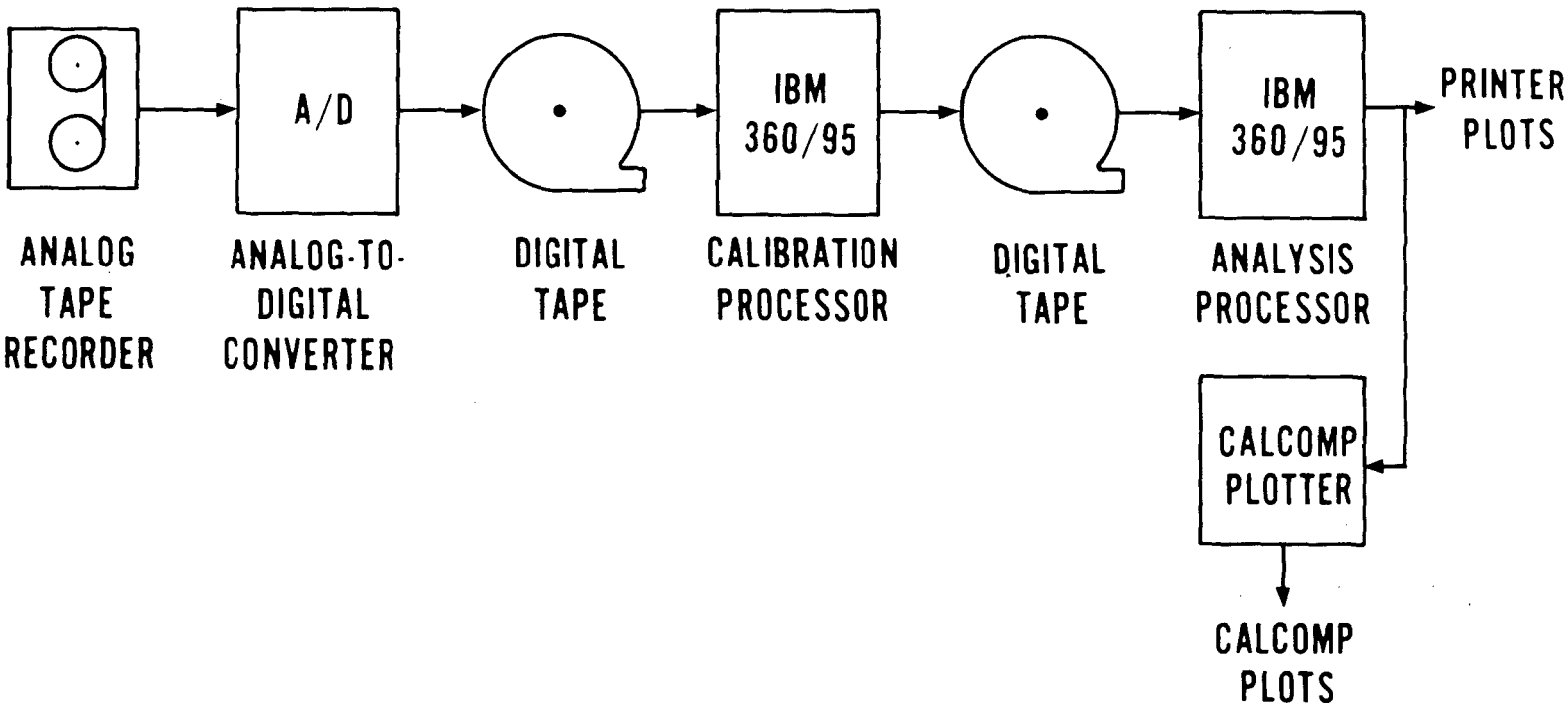

Figure 4. Data-Reduction Configuration

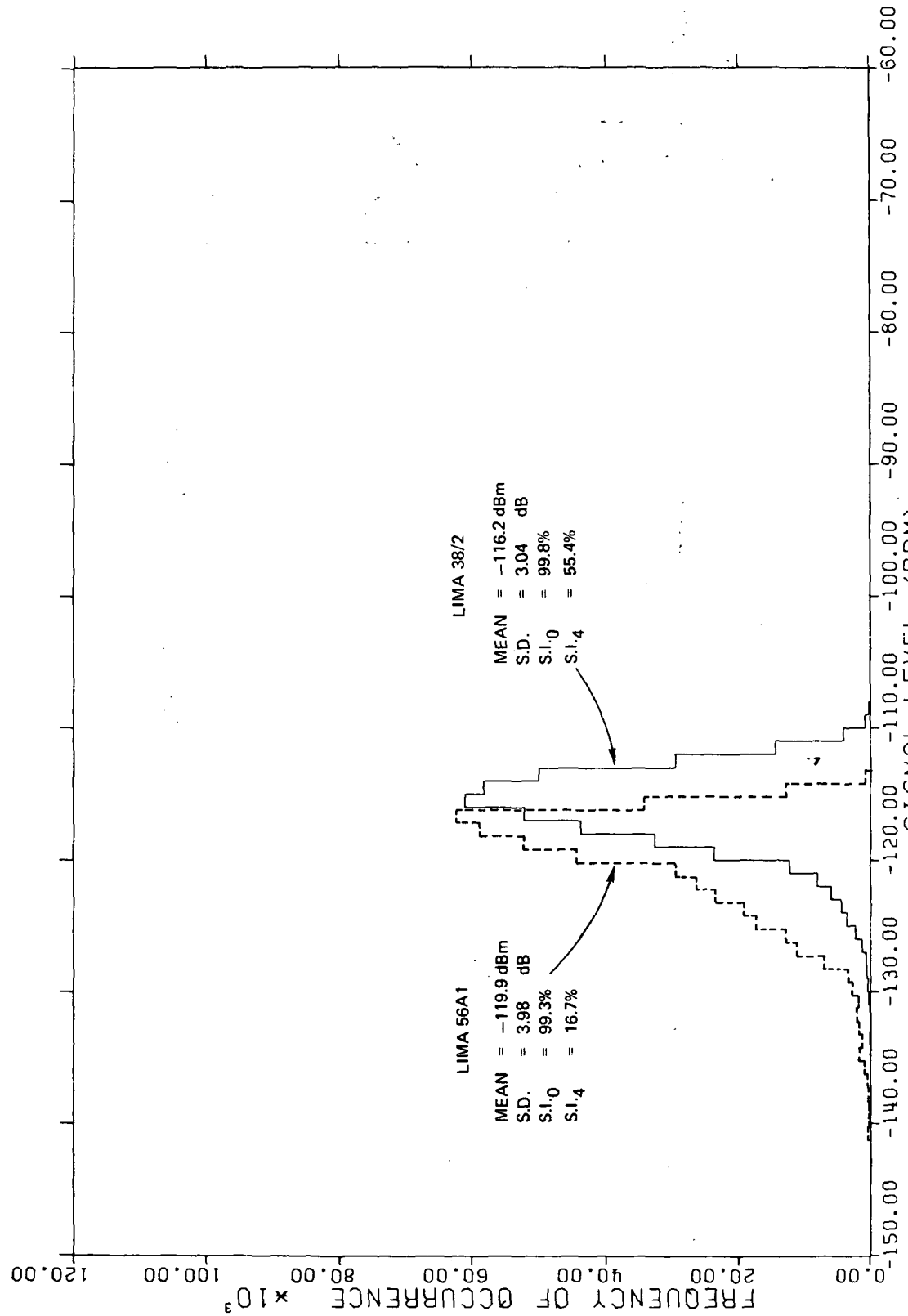

Figure 5. Frequency Distribution of Scintillation

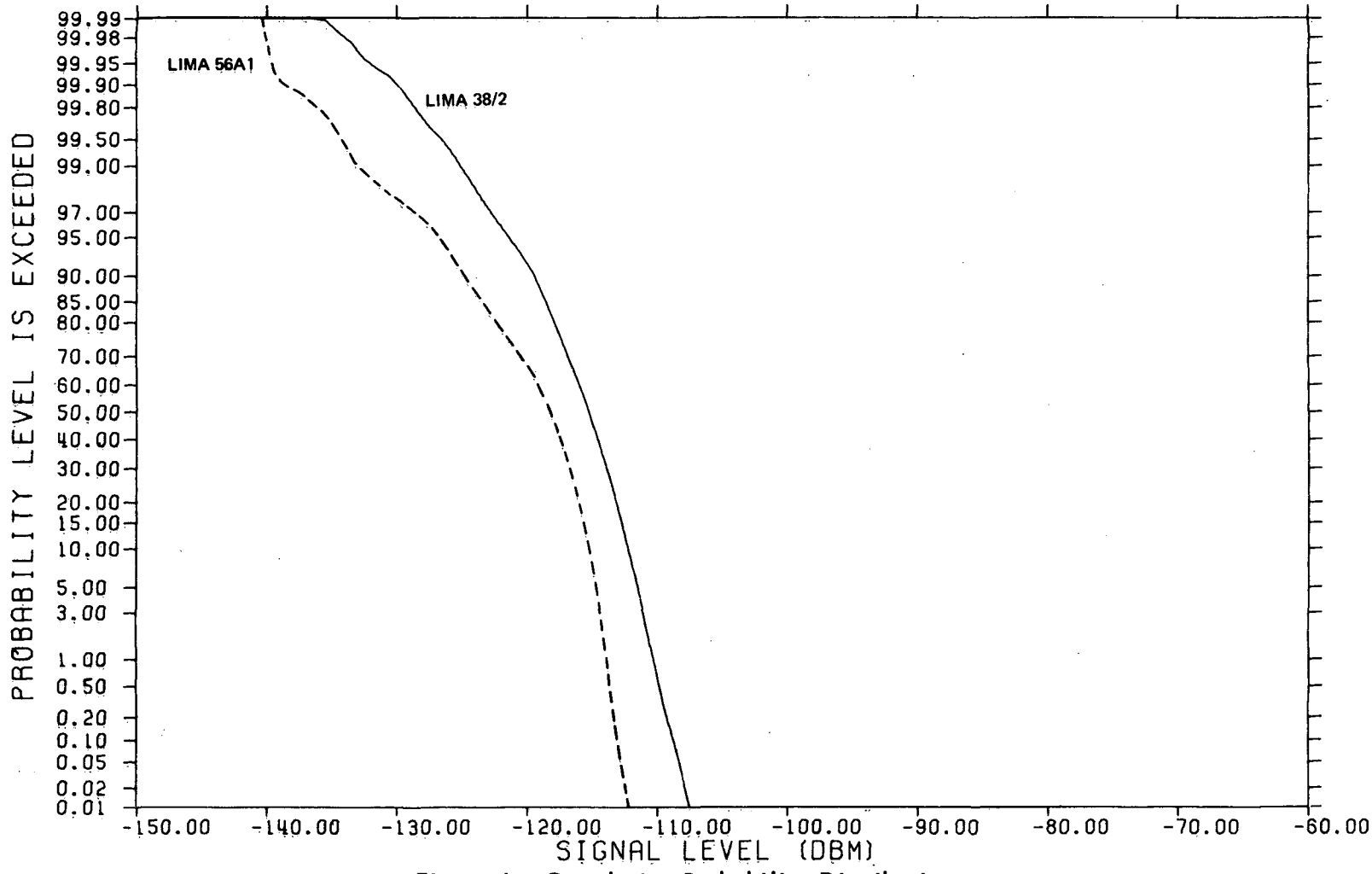

Figure 6. Cumulative Probability Distributions

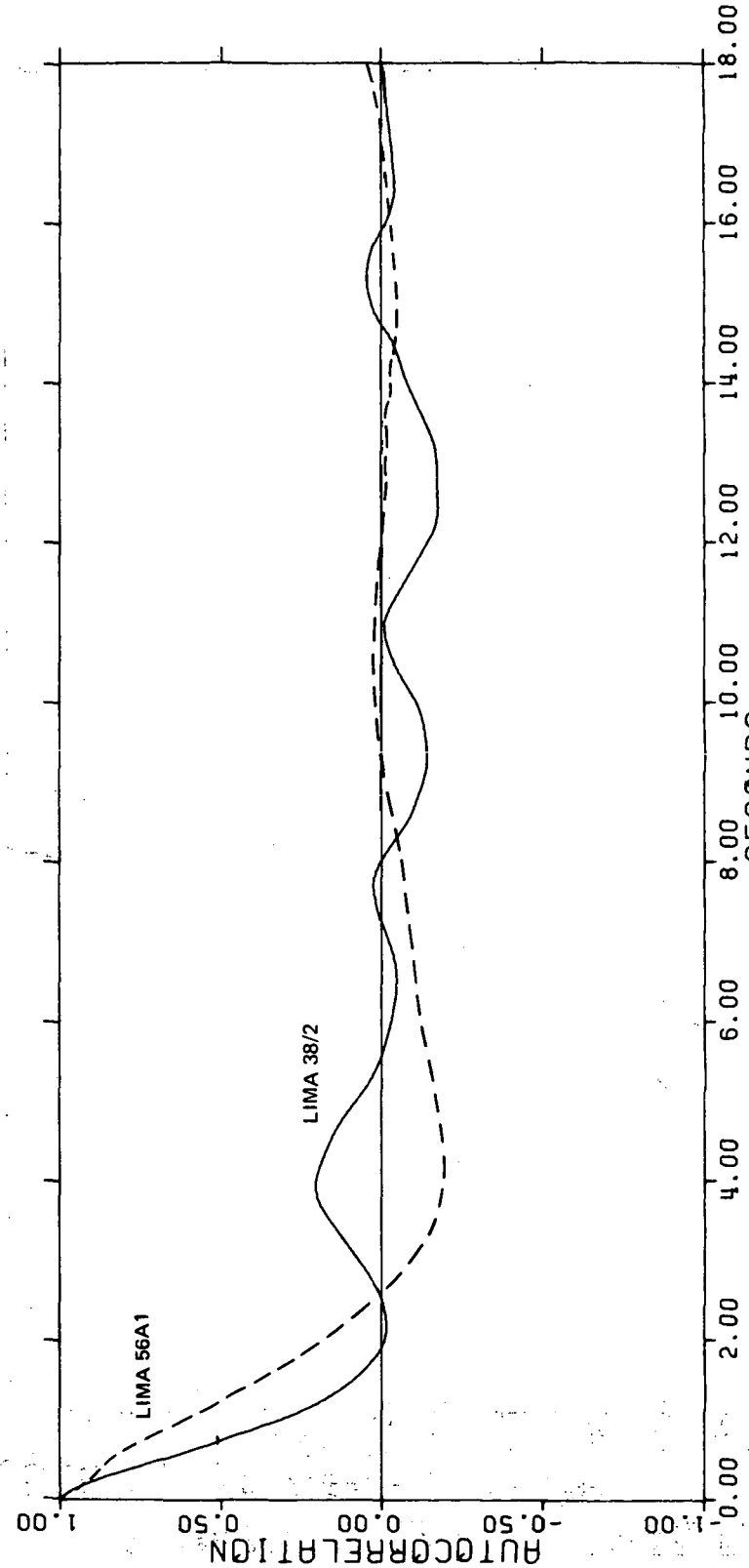

Figure 7. Autocorrelation of Scintillation

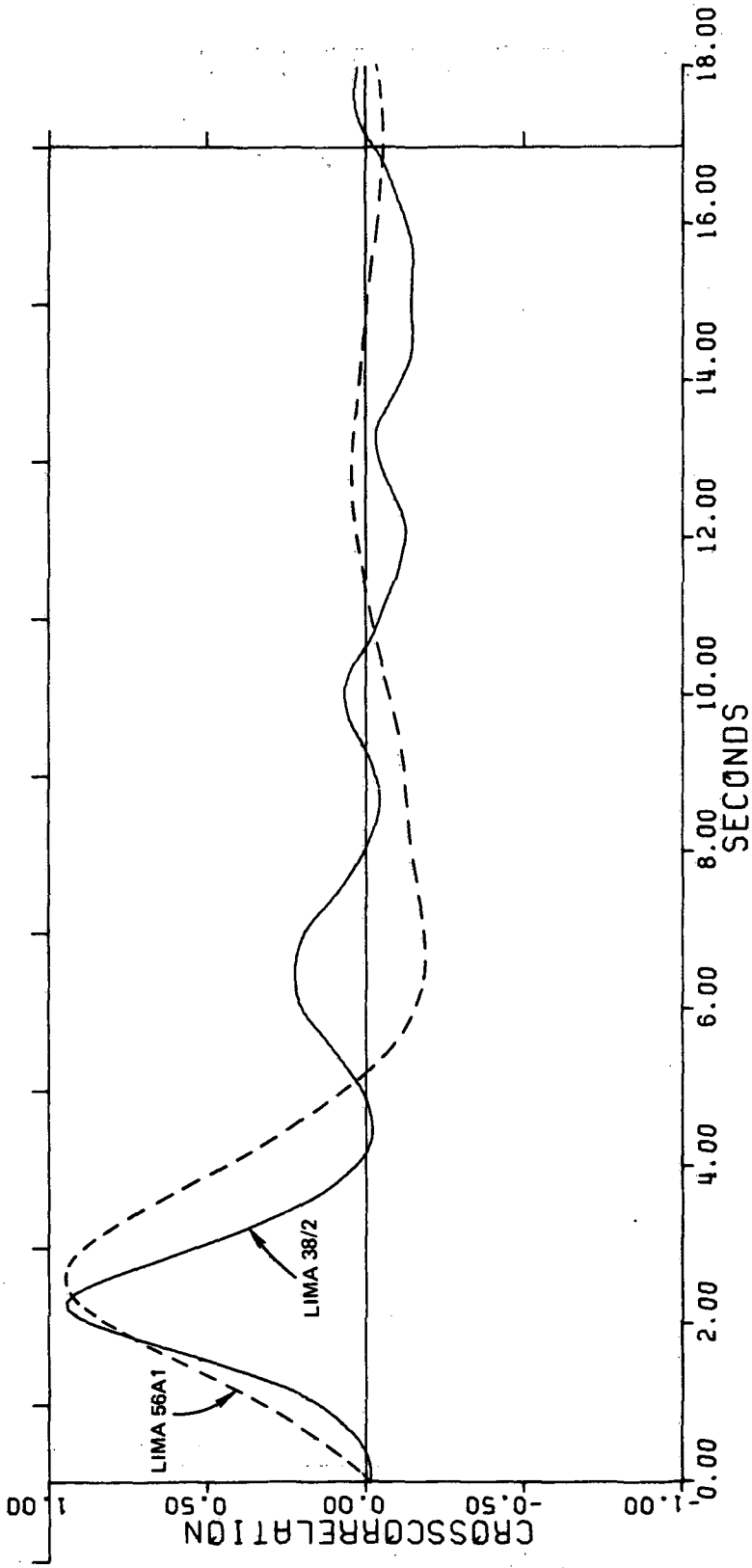

Figure 8. East-West Crosscorrelation of Scintillation

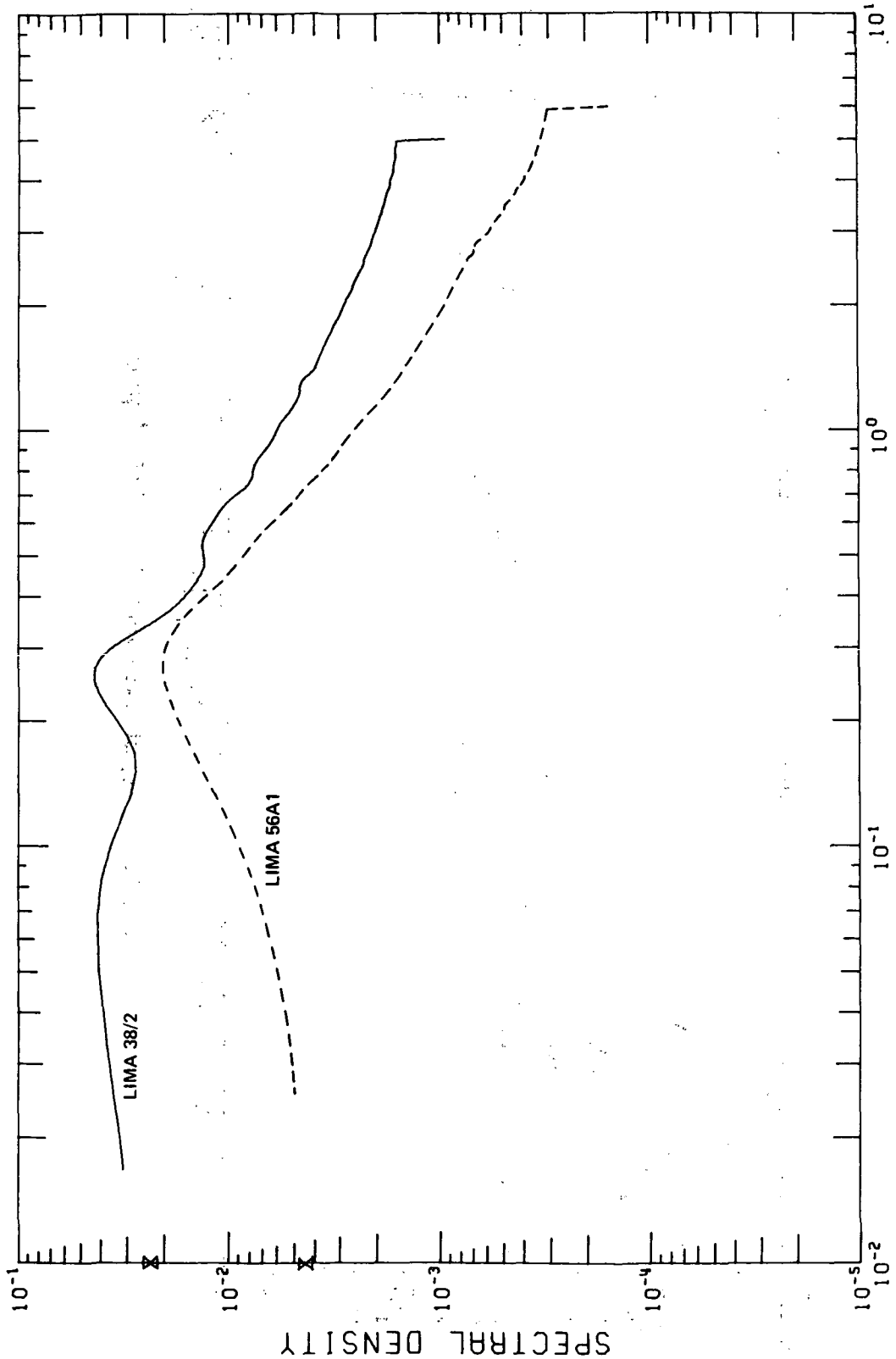

Figure 9. Power Spectral Density of Scintillation

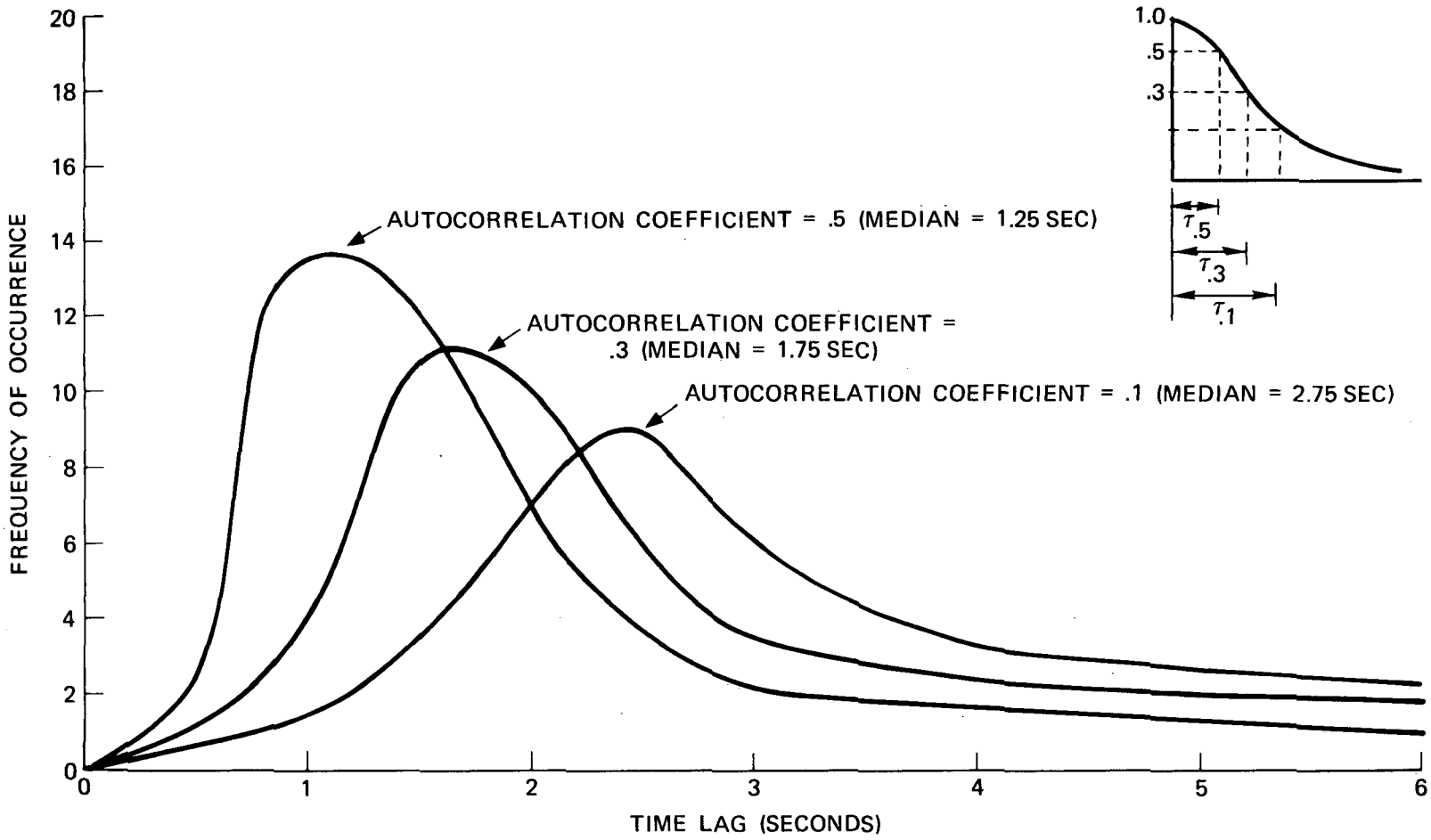

Figure 10. Probability Density Functions of Three Autocorrelation Coefficients

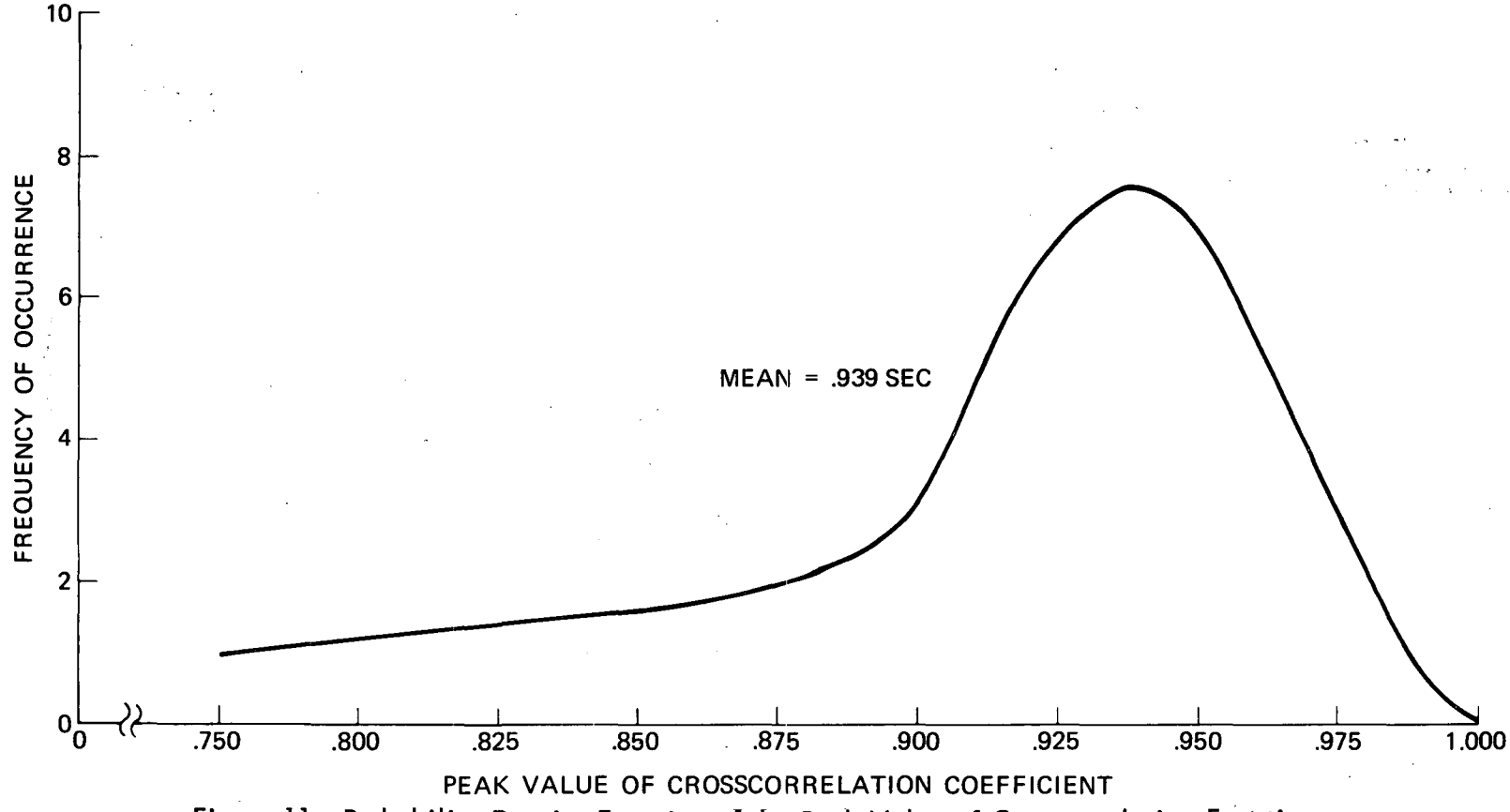

Figure 11. Probability Density Function of the Peak Value of Crosscorrelation Functions

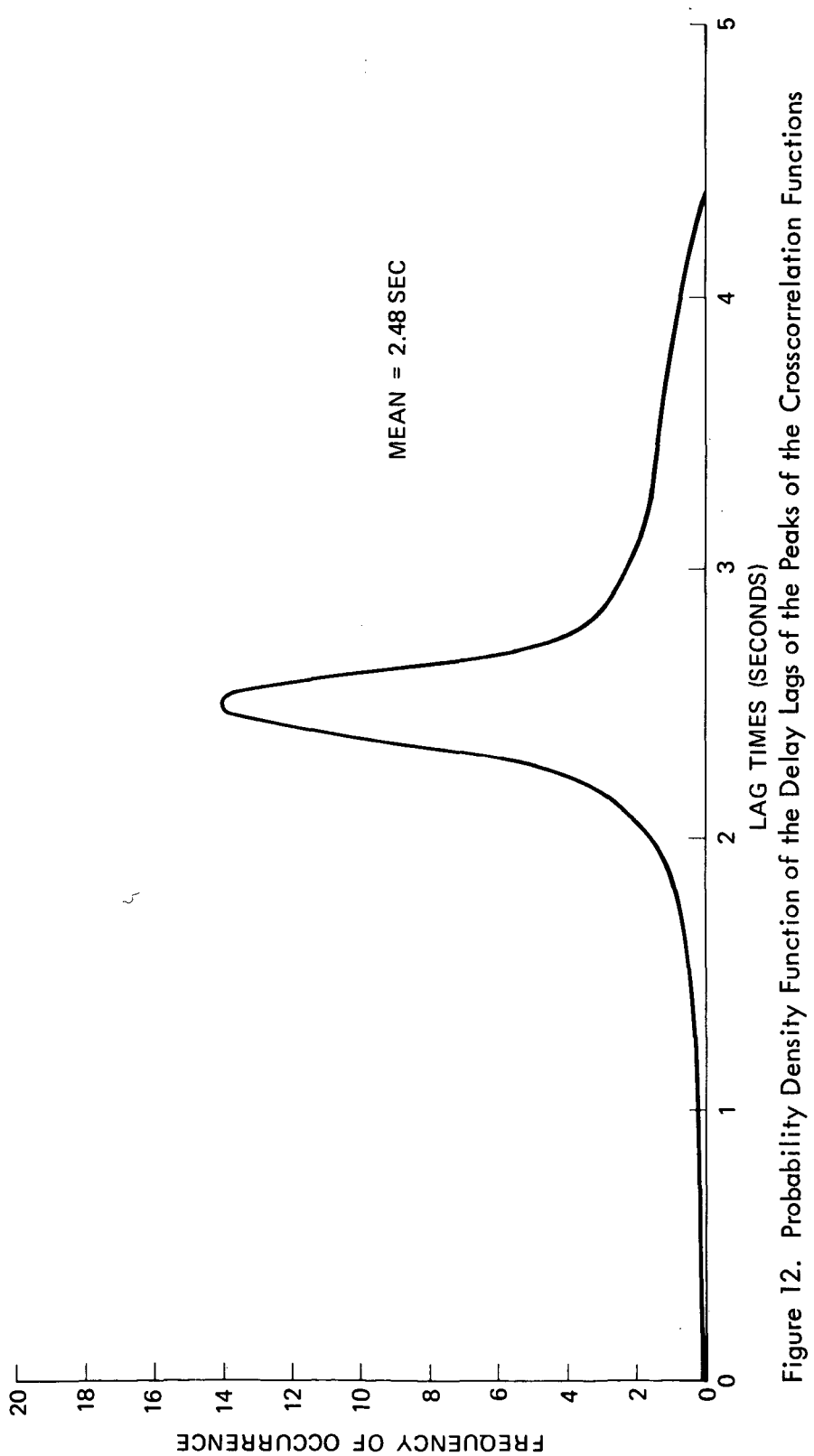

Figure 12. Probability Density Function of the Delay Lags of the Peaks of the Crosscorrelation Functions

* U.S. GOVERNMENT PRINTING OFFICE: 1972—738-963/211